J Membrane Biol (2015) 248:1079–1087
DOI 10.1007/s00232-015-9821-x

Effect of Erythrodiol, A Natural Pentacyclic Triterpene from Olive Oil, on the Lipid Membrane Properties

Lamice Habib[1,2] · Alia Jraij[1] · Nathalie Khreich[1] · Catherine Charcosset[2] · Hélène Greige-Gerges[1]

Received: 13 February 2015 / Accepted: 25 June 2015 / Published online: 4 July 2015

Abstract The effect of erythrodiol, a natural pentacyclic triterpene to which humans are exposed through nutrients, on the lipid membranes is studied using liposomes as a membrane model. Empty and erythrodiol-loaded liposomes were prepared by the reverse phase evaporation method followed by the extrusion and by the thin film hydration method. Liposomes were characterized in terms of size and zeta potential and were imaged by transmission electron microscopy (TEM) and atomic force microscopy (AFM). The effect of erythrodiol on thermotropic behavior of DPPC bilayers is also examined by differential scanning calorimetry (DSC). The DSC thermograms suggested that erythrodiol interacted with the polar head groups of phospholipids and may produce a disruption of the ordering of the alkyl chains. The diffraction light scattering analysis showed that erythrodiol-loaded liposomes presented a decrease in the vesicle size when compared to blank liposomes. Images obtained by TEM confirmed the formation of unilamellar and spherical liposomes. AFM images showed spherical vesicles and single lipid bilayers. The latter were more abundant in the preparations containing erythrodiol than in the blank ones. Moreover, erythrodiol-loaded liposomes tended to rupture into single lipid bilayers during scanning. The study may provide a better understanding of pentacyclic triterpenes–membrane interaction.

Keywords Atomic force microscopy · Differential scanning calorimetry · Dynamic light scattering · Erythrodiol · Liposomes · Transmission electron microscopy

Introduction

Erythrodiol (18β-olean-12-ene-3β,28diol) (Fig. 1), is a pentacyclic triterpenic compound. It is a precursor of oleanolic acid and its isomer maslinic acid in plants (Stiti et al. 2007). Oleanolic acid derivatives were used for medicinal purposes in many Asian countries (Setzer and Setzer 2003; Ovesna et al. 2004). A special source of these secondary metabolites is "orujo" olive oil, which is obtained from the waste of olives, skin, and seeds after cold-press extraction of virgin olive oil. This product is rich in pentacyclic triterpenoids and contains erythrodiol in concentrations up to 690 mg/kg (Perez-Camino and Cert 1999; Albi et al. 1986). Numerous studies described the wide range of erythrodiol biological activities (Sánchez-Quesada et al. 2013). Erythrodiol has proven to be effective in skin chronic inflammation (Manez et al. 1997). It has an inhibitory action against tumor promoter (Nishino et al. 1988) and shows remarkable suppressive effects on skin tumor formation in mice (Nishino et al. 1988). Erythrodiol exerted high cytotoxicity against human HO-8910 ovarian carcinoma and human SMMC-7721 hepatocarcinoma cell lines (Yang et al. 2009), and demonstrated antiproliferative and apoptotic activity toward HT-29 human colon adenocarcinoma cells (Juan et al. 2008), human MCF-7 breast cancer cell line (Allouche et al. 2011), and human 1321N1

✉ Hélène Greige-Gerges
hgreige@ul.edu.lb; greigegeorges@yahoo.com

[1] Bioactive Molecules Research Group, Doctoral School of Sciences and Technologies, Department of Chemistry and Biochemistry, Faculty of Sciences-2, Lebanese University, B.P. 90656, Jdaidet El-Matn, Lebanon

[2] Laboratoire d'Automatique et de Génie des Procédés (LAGEP), UMR 5007, CNRS, CPE, 43 bd du 11 Novembre, 691622 Villeurbanne Cedex, France

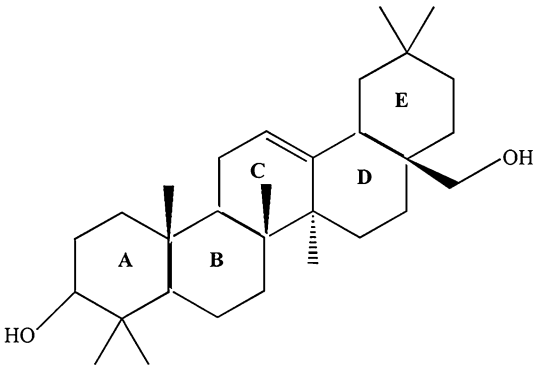

Fig. 1 Chemical structure of erythrodiol

astrocytoma cell line (Martín et al. 2009). It was recently reported that erythrodiol has antioxidant and cytotoxic activities against HEPG2 liver cancer cell line (Gedara and Galala 2014).

The vasorelaxant and cardioprotective activities of erythrodiol have been reported in many studies (Rodríguez-Rodríguez et al. 2004; Rodriguez-Rodriguez et al. 2006; Allouche et al. 2010; Lou-Bonafonte et al. 2012). Erythrodiol is able to relax, in a concentration-dependent manner, the contractions induced by phenylephrine in rat aortic rings with functional endothelium (Rodríguez-Rodríguez et al. 2004). Moreover, diol triterpenes, erythrodiol, and uvaol, block profibrotic effects of angiotensin II and protect the cardio-vascular system from cardiac hypertrophy (Martín et al. 2012a). Besides, erythrodiol and oleanolic acid protect against experimental autoimmune encephalomyelitis, which is an animal model for brain inflammation, by restricting infiltration of inflammatory cells into the central nervous system (Martín et al. 2012b).

It is well established that natural triterpenes interact with the lipid membrane and affect its properties. Cholesterol, ergosterol, and stigmasterol are membrane constituents; they insert deeply in the membrane structures and affect their dynamic properties (Dufourc 2008). The structure of a triterpenic compound (Dufourc 2008; Prades et al. 2011; Rodriguez et al. 1997), the number of oxidized groups (Massey and Pownall 2005, 2006), and the conjugation to a sugar structure (Lorent et al. 2013; Hu et al. 1996) are the factors that control the interaction and consequently the effects of triterpenic molecules on the membrane properties. Among the natural pentacyclic triterpenes, many reports have been published concerning the interaction with lipid membrane of lupeol (Rodriguez et al. 1997; Broniatowski et al. 2012a, b), betulinic acid (Broniatowski et al. 2012a, b), betulin (Broniatowski et al. 2012a), oleanolic, maslinic, ursolic acids (Prades et al. 2011; Han et al. 1997), alpha-amyrin, and taraxerol (Rodriguez et al. 1997).

In this study we examine the effect of a pentacyclic triterpenic diol, erythrodiol, on the physicochemical properties of the lipid bilayer using liposomes as artificial model membrane. Thus, large unilamellar vesicles (LUV) were prepared in the absence and presence of erythrodiol at different concentrations using the reverse phase evaporation technique. Different techniques such as dynamic light scattering (DLS), transmission electron microscopy (TEM), and atomic force microscopy (AFM) were performed in order to investigate the effects of erythrodiol on the size and morphology of lipid vesicles. Moreover, differential scanning calorimetry (DSC) was used to determine the thermodynamic parameters of DPPC-blank and erythrodiol-loaded multilamellar vesicles prepared by the thin film hydration technique.

Materials and Methods

Chemicals

Cholesterol (Cho) (purity 99 %), phosphotungstic acid hydrate, trizma base, and the organic solvents: chloroform, methanol, diethyl ether, and hydrochloric acid were purchased from Sigma-Aldrich, France. Dipalmitoylphosphatidylcholine (DPPC), dipalmitoyl phosphatidylethanolamine (DPPE), and dipalmitoyphosphatidylglycerol (DPPG) were purchased from Lipoid AG, Switzerland. Erythrodiol (purity 97 %) was obtained from Extrasynthèse, Genay, France.

Liposomes Preparation by Reverse Phase Evaporation Method

The reverse phase evaporation method was used to prepare liposomes. A lipid mixture, 50 µmol, of DPPC/DPPG/DPPE/Cho (5/0.5/0.25/5 molar ratio) (batch 1) was dissolved in 5 ml of a solvent mixture of chloroform, diethyl ether, and methanol (6/6/1, v/v/v) (Habib et al. 2013, 2014). The solution was sonicated (Bandelin Sonorex) for 1 min at 60 °C under nitrogen to avoid lipid oxidation. Then 0.75 ml of 0.1 M Tris–HCl buffer (pH 7.4) was added, followed by sonication for 6 min at 60 °C under nitrogen. The organic solvents were removed at 45 °C, by a rotary vacuum evaporator (BÜCHI Rotavapor R-124). In the last step, 0.1 M Tris–HCl buffer (pH 7.4) (1.5 ml) was added and the mixture was sonicated for 5 min at 60 °C under nitrogen.

The prepared liposomes were then incubated in a water bath at 60 °C for 35 min and underwent extrusion through polycarbonate filters using a mini extruder (Avanti Polar Lipids, Switzerland). Thereby, liposomes were forced to pass through polycarbonate membranes (Avanti Polar

Lipids, Switzerland) of decreasing pore size (ten times through a 1-μm pore size membrane followed by ten times through a 0.4-μm pore size membrane). The solution was ultracentrifuged (Beckman Coulter, Optima^{TM} MAX-XP ultracentrifuge) at 50,000×*g* for 30 min at 4 °C and the obtained pellet was finally suspended in 2 ml of 0.1 M Tris–HCl buffer (pH 7.4).

Using the previous protocol, liposomes were prepared in the presence of 1.0 mg and 2.5 mg of erythrodiol (batches 2 and 3 respectively). The total molar ratio of phospholipids was maintained constant and erythrodiol was added to the lipid mixture at the expense of cholesterol. The corresponding molar ratios of phospholipids/Cho/erythrodiol were, respectively, 5.75/4.5/0.5 and 5.75/3.8/1.2 for batches 2 and 3. Every batch was prepared three times.

Liposome Characterization

Liposome Size

Dynamic light scattering (DLS), also known as photon correlation spectroscopy, was used to determine the size and the size distribution of liposomes. In this study, a Malvern Zetasizer Nano-series (Malvern Instruments Zen 600, Malvern, UK) was used. The data on particle size distribution were collected using the DTS (nano) software provided with the instrument. Aliquots from resuspended pellets of various batches were diluted 10-fold with the buffer Tris–HCl (0.1 M, pH 7.4). All measurements were performed in triplicate at 25 °C. The results were calculated as mean ± standard deviation. The polydispersity index (PdI), which is an indicator of the particle size distribution of a sample, was also determined. It ranges from 0 (monodispersed) to 1 (broad distribution).

Zeta Potential

The zeta potential was determined using the Malvern Zetasizer Nano-series and was calculated from the electrophoretic mobility by the Helmholtz–Smoluchowski equation (Hunter et al. 2001). Measurements on resuspended pellet for all batches of liposomes were performed in triplicate. The samples were diluted 10 times with the Tris–HCl buffer. The results were reported as mean ± standard deviation.

Transmission Electron Microscopy

Liposome suspensions (batches 1, 2, and 3) were imaged using a transmission electron microscope (TEM) (Philips CM120; Eindhoven, Netherlands). A drop of ten times buffer-diluted liposome suspension was placed onto a 200-mesh formvar carbon-coated copper grid, forming a thin liquid film. The films were negatively stained with a 2 % phosphotungstic acid solution left in contact with the sample for 2 min. The excess of the phosphotungstic acid solution was then removed with a filter paper and the samples were dried at room conditions before the vesicles were imaged at an electron acceleration voltage of 80 kV.

Atomic Force Microscopy

Atomic force microscopy (AFM) experiments were carried out with a commercial AFM (Multimode Nanoscope, Bruker). Mica sheets were freshly cleaved to obtain a flat and uniform surface and were used as the substrate for AFM observation. Before the deposition of the sample on the substrate, mica sheets were treated with a solution of nickel chloride 10 mM to compensate the negative charges of the mica in order to promote the adsorption of the negatively charged liposomes. Thus, 100 μl of the nickel chloride solution was deposited on the mica surface and incubated for 10 min at room temperature. Then the substrate was washed three times with ultrapure water to eliminate the excess of the solution. After that, an aliquot of 100 μl of the resuspended pellet from each batch was immediately placed on the mica surface and incubated for 30 min at room temperature. The sample was thereafter washed three times with ultrapure water to eliminate non-adsorbed vesicles. AFM contact mode images were captured in ultrapure water with a biolever Olympus (spring constant 0.006 N/m) over a selected area in the dimension of 5 μm × 5 μm. Images were acquired at 90° scan angle with a scan rate of 2 Hz. The tip velocity was set at 20 μm/s and the applied force was maintained as low as possible. The height and the size of the liposomes were measured using the Nanoscope V613r1 software.

Lipid Bilayer Thermodynamic Parameters

Preparation of Multilamellar Vesicles (MLV)

Erythrodiol-loaded MLV were prepared by the thin film hydration technique (Bangham et al. 1965). DPPC (50 mg) was mixed with erythrodiol at molar ratios DPPC:erythrodiol of 100:10, 100:17, and 100:34. The components were dissolved in a 2:1 (v/v) solvent mixture of chloroform/methanol (10 mL). The solvent was evaporated using a rotary evaporator at 55 °C to obtain a thin film of dried lipid. The film was then hydrated with 2 ml of 0.1 M Tris–HCl (pH 7.4). The final DPPC concentration was 25 mg/mL. The preparations were alternatively vortexed for 5 min and warmed in a water bath at 55 °C for 5 min. The cycle was repeated three times. Unloaded DPPC liposomes were prepared as control.

Differential Scanning Calorimetry (DSC)

Thermal scans were carried out using a DSC Q200 scanning calorimeter (TA instruments). An empty hermetically sealed aluminum pan was used as reference. 10 µl of MLV liposome suspension was carefully set in the aluminum hermetic pan, which was then sealed. Samples were run at a scan rate of 5 °C/min in a temperature range of 20–50 °C. Samples were scanned at least ten times until obtaining identical and reproducible thermograms. DSC data were analyzed with the instrument software package. The measured parameters were the transition temperature (T_m) determined from the maximum of the recorded heat capacity, transition enthalpy (ΔH_m) obtained from the area under the peak, and the respective parameters for the pre-transition (T_p and ΔH_p).

Results

Determination of Liposome Size and Zeta Potential

The DLS technique was used to measure the size, size distribution, and zeta potential of empty and erythrodiol-loaded liposomes. The obtained values revealed that the empty liposomes have a mean diameter equal to 364 ± 17 nm, which is close to the pore size of the last membrane they were extruded through (Table 1). However, liposomes incorporating erythrodiol were smaller and had a mean diameter around 213 ± 42 and 186 ± 7 nm for batches 2 and 3, respectively (Table 1). The polydispersity index (PdI) for all batches was around 0.2 indicating that the liposome populations were homogeneous and had a narrow size distribution (Table 1). The obtained zeta potential measurements showed that there is no important difference between zeta potential values of empty and erythrodiol-loaded liposomes (Table 1).

TEM Images of Liposomes

TEM was performed to visualize liposomes prepared in the absence (batch 1) and presence (batches 2 and 3) of erythrodiol. Clear transmission electron micrographs of the vesicles were obtained using the phosphotungstic acid as contrastant (Fig. 2).

The negative-stain TEM images revealed nanometric-sized liposomes in accordance with the DLS measurements (Fig. 2). They confirmed the presence of well-identified unilamellar spherical vesicles with a large internal space for all batches (Fig. 2). Figure 2a–c are the transmission electron micrographs of vesicles from batches 1, 2, and 3, respectively.

AFM Images of Liposomes

AFM was used to investigate the effect of erythrodiol on the morphology of DPPC/DPPG/DPPE/Cho lipid vesicles. In accordance with TEM images, the AFM images of liposomes from batches 1, 2, and 3 showed that empty and erythrodiol-loaded liposomes had spherical shapes (black arrows, Fig. 3). In addition to the spherical vesicles, AFM images of each batch revealed the presence of single lipid bilayers of 5 nm in height on the modified mica (white arrows, Fig. 3). These single lipid bilayers became more frequent during scanning. They were formed by the rupture of the soft vesicles under the tip effect and/or by the fusion of two closed single lipid bilayers to form a bigger patch of 5 nm in height (data not shown).

Figure 3a–c show respectively, the AFM images of batches 1, 2, and 3. For empty liposomes (batch 1), Fig. 3a revealed the presence of spherical vesicles and some single lipid bilayers of 5 nm height. It is noteworthy that the intact vesicles of Fig. 3a were of different dimensions and their number exceeded that of single lipid bilayers. For erythrodiol-loaded liposomes of batch 2, Fig. 3b shows from the beginning of the scan, an important number of big patches of single lipid bilayers that grew during the scan. Also in the same batch, many spherical and intact vesicles persist on the substrate. For erythrodiol-loaded liposomes of batch 3, single lipid bilayers were more frequent than intact vesicles from the beginning of the scan (Fig. 3c). It is remarkable that in the presence of erythrodiol, the formation of single lipid bilayers and their patches were much higher. In order to confirm this effect, we prepared an

Table 1 Measurements of size, size distribution, and zeta potential by DLS for liposomes of batches 1 (phospholipids/cho/erythrodiol 5.75/5/0), 2 (phospholipids/cho/erythrodiol 5.75/4.5/0.5), and 3 (phospholipids/cho/erythrodiol 5.75/3.8/1.2)

Batches	Phospholipids/Cho/erythrodiol	Diameter (nm) ± SD	PdI ± SD	Zeta potential (mV) ± SD
Batch 1	5.75/5/0	364 ± 17	0.23 ± 0.04	−14.9 ± 0.8
Batch 2	5.75/4.5/0.5	213 ± 42	0.22 ± 0.10	−14.7 ± 0.7
Batch 3	5.75/3.8/1.2	186 ± 7	0.19 ± 0.01	−16.4 ± 0.8

Values are expressed as mean ± SD

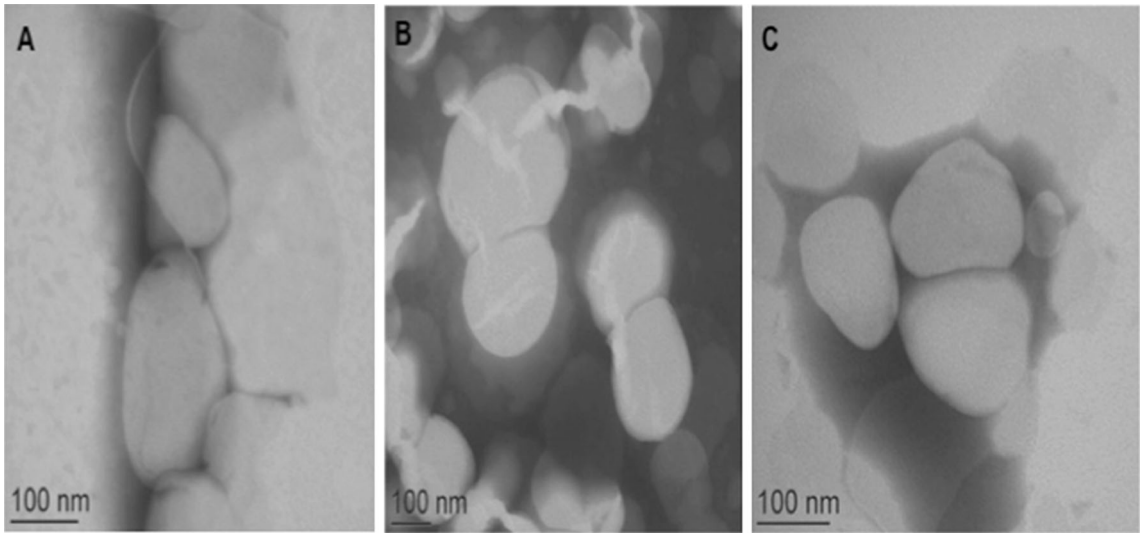

Fig. 2 Images obtained by transmission electron microscopy of **a** Batch 1 (DPPC/DPPG/DPPE/Cho/erythrodiol 5/0.5/0.25/5/0), **b** batch 2 (DPPC/DPPG/DPPE/Cho/erythrodiol 5/0.5/0.25/4.5/0.5), and **c** batch 3 (DPPC/DPPG/DPPE/Cho/erythrodiol 5/0.5/0.25/3.2/1.8)

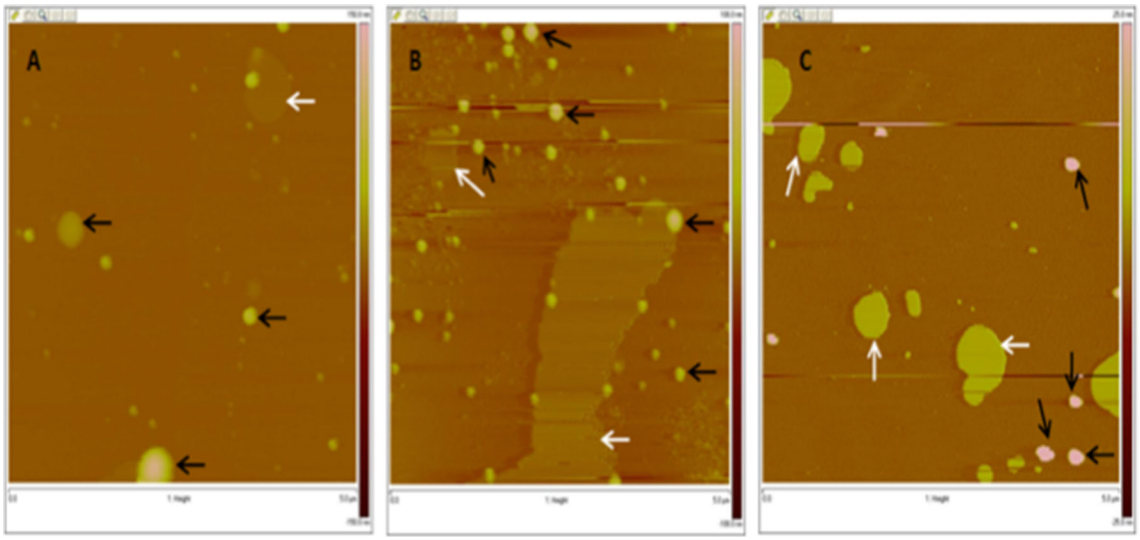

Fig. 3 AFM contact mode images of vesicles from **a** Batch 1 (DPPC/DPPG/DPPE/Cho/erythrodiol 5/0.5/0.25/5/0), **b** batch 2 (DPPC/DPPG/DPPE/Cho/erythrodiol 5/0.5/0.25/4.5/0.5), and **c** batch 3 (DPPC/DPPG/DPPE/Cho/erythrodiol 5/0.5/0.25/3.8/1.2), taken over an area of 5 μm × 5 μm. *Black* and *white arrows* refer, respectively, to vesicles and SLBs

additional batch of LUV containing a higher quantity of erythrodiol (DPPC/DPPG/DPPE/Cho/erythrodiol 5/0.5/0.25/3/2). The AFM images showed that the mica surface was completely covered by patches of single lipid bilayers of 5 nm of height simultaneously with an important number of intact vesicles (Fig. 4).

The dimensions of the observed vesicles were measured. The diameters ranged from 250 to 500 nm for liposomes of batch 1 and from 200 to 250 nm for those of batches 2 and 3. The vesicles were smaller in the presence of erythrodiol. Besides, the height of the vesicles was measured. For the three batches, liposomes height varied between 25 and 150 nm and no difference was observed between empty and erythrodiol-loaded liposomes.

Effect of Erythrodiol on the Lipid Bilayer Thermotropic Behavior

In this study, the thermotropic behavior of DPPC bilayers prepared in the absence and presence of erythrodiol at various molar ratios of DPPC:erythrodiol was determined by DSC (Fig. 5; Table 2).

DPPC bilayer showed a lamellar gel ($L_{\beta'}$) to rippled gel ($P_{\beta'}$) phase transition ($T_p = 36 \pm 1$ °C and

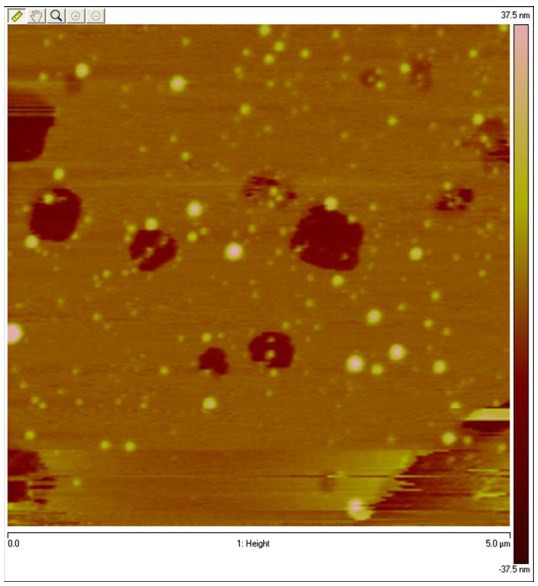

Fig. 4 AFM contact mode images of vesicles obtained at high erythrodiol concentration (DPPC/DPPG/DPPE/Cho/erythrodiol 5/0.5/0.25/3/2) taken over an area of 5 µm × 5 µm

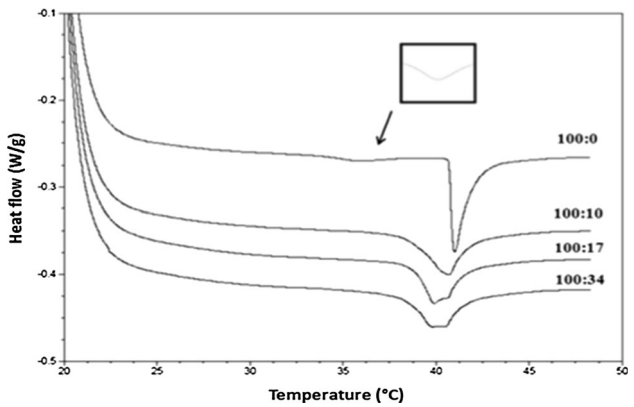

Fig. 5 DSC thermograms of DPPC bilayers at molar ratios of DPPC:erythrodiol 100:0, 100:10, 100:17, and 100:34

$\Delta H_p = 2.38 \pm 0.98$ kJ/mol) and then to lamellar liquid crystalline (L_α) phase transition ($T_m = 40.83 \pm 0.58$ °C and $\Delta H_m = 46.61 \pm 3.59$ kJ/mol) (Fig. 5; Table 2). The main effects of erythrodiol on the DSC thermograms of the DPPC bilayers were a disappearing of the pre-transition peak associated to the $L_{\beta'}$-to-$P_{\beta'}$, and a broadening followed by a splitting of the transition peak associated with the $P_{\beta'}$-to-L_α phase transition (Fig. 5). The peak shape of $P_{\beta'}$-to-L_α phase transition revealed an increase in the bilayer asymmetry. At concentrations of 17 and 34 %, erythrodiol induced the splitting of the main transition peak into two peaks, T_{m1} and T_{m2} (Table 2). T_{m1} is close to the T_m of the empty DPPC bilayers while T_{m2} is lower.

In addition, the total transition enthalpy was decreased in the presence of erythrodiol. The obtained values were 46.61 ± 3.59, 29.67 ± 3.89, 26.29 ± 4.60, and 31.21 ± 3.73 kJ/mol, respectively, for DPPC:erythrodiol 100:0, 100:10, 100:17, and 100:34 (Table 2). The peak shape was highly broadened at erythrodiol concentration of 17 and 34 % rendering difficult the calculation of ΔH_{m1} and ΔH_{m2}.

Discussion

In this work, we studied the interaction of a pentacyclic triterpenic diol structure, erythrodiol, with lipid membrane. Erythrodiol is widely distributed in the Mediterranean diet mainly in olive oil and exhibits numerous biological properties. Empty and erythrodiol-loaded liposomes were prepared and characterized in terms of size, size distribution, morphology, and thermotropic phase behavior.

Thermodynamic states and phase transition temperatures of lipid bilayer membrane are considered as an important physicochemical index in assessing the bilayer structure (Demetzos 2008). DSC thermograms enable the determination of the changes of the lipid bilayers phase transitions produced by the incorporation of a molecule in the liposomal structure (Elhissi et al. 2006; Cong et al. 2009). The obtained values of the T_p and T_m of the empty DPPC liposomes were in good agreement with the literature (Biruss et al. 2007; El Maghraby et al. 2005; Zhao and Feng 2005). In the presence of erythrodiol, the pre-transition peak disappeared. The pre-transition from the gel phase ($L_{\beta'}$) to the rippled phase ($P_{\beta'}$) is related to the polar region of the lipid bilayer; it is associated to an interaction with the polar head groups of phospholipids or to a change in their orientation (Heimburg 2000). Our results suggest

Table 2 Thermotropic parameters obtained by DSC for all prepared batches of DPPC:Erythrodiol 100:0, 100:10, 100:17, and 100:34

DPPC:Erythrodiol	T_p (°C) ± SD	ΔH_p (KJ/mol) ± SD	T_{m1} (°C) ± SD	T_{m2} (°C) ± SD	ΔH_m (KJ/mol) ± SD
100:0	36 ± 1	2.38 ± 0.98	40.83 ± 0.58		46.61 ± 3.59
100:10			40.29 ± 0.50		29.67 ± 3.89
100:17			40.71 ± 0.04	39.92 ± 0.07	26.29 ± 4.60
100:34			40.53 ± 0.06	39.85 ± 0.08	31.21 ± 3.73

Values are expressed as mean ± SD

that erythrodiol interacts with the polar head groups of membrane constituents. The variation of the calorimetric parameters of the main transition is usually attributed to the incorporation of the molecule into the hydrophobic core of the lipid bilayer. At molar ratio DPPC:erythrodiol of 10 %, the shape of the transition peak became shorter and broader. The broadening of the peak reflects an increase in the bilayer asymmetry. At molar ratios DPPC:erythrodiol of 17 and 34 %, a splitting of the transition peak is produced indicating the disruption of the ordering of the alkyl chains. The decrease of the transition enthalpy in the presence of a drug is usually attributed to the drug interaction with the hydrophobic chains of the bilayer (Detoni et al. 2009; Koukoulitsa et al. 2011; Potamitis et al. 2011; Barenholz et al. 2011). Compared to other pentacyclic triterpenes (Prades et al. 2011) which did not affect significantly the melting temperature and the enthalpy of the main phase transition, erythrodiol produced remarkable decrease of the enthalpy values of the main peak (Table 2). Rodriguez et al. (1997) demonstrated that cholesterol and α-amyrin, unlike other pentacyclic monoalcohols, are incorporated at high levels into DPPC bilayers and this was attributed to their planarity. The chemical/structural parameters of triterpenic molecules that control their interaction with membranes should be defined through a structure–activity relationship.

Size measurements obtained by DLS revealed that the incorporation of erythrodiol in the liposomes produced a decrease in the liposomes size. Many previous studies have demonstrated that the size of liposomes was decreased in the presence of diterpene structures like labdanes (Matsingou et al. 2005) and monoterpene ones like essential oils (Detoni et al. 2009; Sinico et al. 2005; Valenti et al. 2001; Yoshida et al. 2010). The PdI values revealed the homogeneity of the liposomal populations as it was expected upon the extrusion step (Berger et al. 2001; Verma et al. 2003). The incorporation of erythrodiol did not affect the zeta potential of the liposomes since erythrodiol is not ionized at the pH of the medium (pH 7.4).

TEM and AFM are two independent microscopic techniques that were used to visualize the effect of erythrodiol on liposomal morphology. AFM could be used as a complementary technique for the measurements of the vesicle dimensions and it is a highly valuable tool to determine the nanomechanical properties of membranes (Redondo-Morata et al. 2012, Tierney et al. 2001). Accordingly with the DLS measurements, the obtained images from both microscopical techniques confirmed the formation of nanometric-sized and spherical-shaped vesicles in the absence and presence of erythrodiol. Similar observations by TEM and AFM were published for PEGylated liposomes incorporating oleanolic acid (Gao et al. 2012).

Erythrodiol-loaded liposomes were smaller than the empty liposomes. Compared to the values determined by DLS measurements, the higher values of size obtained by AFM measurements are due to the compression of the vesicles by the AFM tip during contact mode scanning. In addition to the intact spherical vesicles, AFM images of all batches present variable sizes of single lipid bilayers patches. The single lipid bilayers or otherwise known as single-bilayer disks (Reviakine and Brisson 2000; Jass et al. 2000) or bilayer patches (Richter et al. 2003), exhibit a constant height of 5 nm, whereas the intact vesicles exhibit a height variation of tens of nm (Reviakine and Brisson 2000; Richter et al. 2003). The formation of patches of single lipid bilayers increased during scanning particularly in the presence of erythrodiol. This increase is due to the fusion of the vesicles with the closed single lipid bilayers or the rupture of the vesicles under the AFM-tip effect. The micellarization and/or immiscibility, which could be induced by the pentacyclic triterpenes, in the bilayers may explain the difference between the behavior of blank and erythrodiol-loaded liposomes under AFM imaging.

Conclusion

This study is the first to elucidate the interaction of the natural pentacyclic triterpene, erythrodiol, with the lipid bilayer membrane. DLS, DSC, TEM, and AFM were used to characterize blank and erythrodiol-loaded vesicles. Compared to blank vesicles, erythrodiol-loaded liposomes were smaller and underwent a rupture on the mica substrate. The results can be considered to understand the molecular basis underlying the erythrodiol–membrane interaction.

Acknowledgments The project was supported by the Research Funding Program at the Lebanese University. We thank the Agence Universitaire de la Francophonie and the Lebanese Council for Scientific Research for supporting the scholarship of Lamice Habib.

References

Albi T, Lanzon A, Navas MA (1986) Quantitative-determination of erythrodiol in oils by gas-chromatography with semi capillary columns (wide bore capillary). Grasas Aceites 37:277–281

Allouche Y, Beltran G, Gaforio JJ, Uceda M, Mesa DM (2010) Antioxidant and antiatherogenic activities of pentacyclic triterpenic diols and acids. Food Chem Toxicol 48:2885–2890

Allouche Y, Warleta F, Campos M, Sánchez-Quesada C, Uceda M, Beltrán G, Gaforio JJ (2011) Antioxidant, antiproliferative, and pro-apoptotic capacities of pentacyclic triterpenes found in the skin of olives on MCF-7 human breast cancer cells and their effects on DNA damage. J Agric Food Chem 59:121–130

Bangham AD, Standish MM, Watkins JC (1965) Diffusion of univalent ions across the lamellae of swollen phospholipids. J Mol Biol 13:238–252

Barenholz Y, Bombelli C, Bonicelli MG, di Profio P, Giansanti L, Mancini G, Pascale F (2011) Influence of lipid composition on the thermotropic behavior and size distribution of mixed cationic liposomes. J Colloid Interface Sci 356:46–53

Berger N, Sachse A, Bender J, Schubert R, Brandl M (2001) Filter extrusion of liposomes using different devices: comparison of liposome size, encapsulation efficiency, and process characteristics. Int J Pharm 223:55–68

Biruss B, Dietl R, Valenta C (2007) The influence of selected steroid hormones on the physicochemical behavior of DPPC liposomes. Chem Phys Lipids 148:84–90

Broniatowski M, Flasiński M, Wydro P (2012a) Lupane-type pentacyclic triterpenes in Langmuir monolayers: a synchrotron radiation scattering study. Langmuir 28:5201–5210

Broniatowski M, Flasiński M, Wydro P (2012b) Investigation of the interactions of lupane type pentacyclic triterpenes with outer leaflet membrane phospholipids—Langmuir monolayer and synchrotron X-ray scattering study. J Colloid Interface Sci 381:116–124

Cong W, Liu Q, Liang Q, Wang Y, Luo G (2009) Investigation on the interactions between pirarubicin and phospholipids. Biophys Chem 143:154–160

Demetzos C (2008) Differential scanning calorimetry (DSC), a tool to study the thermal behavior of lipid bilayers and liposomal stability. J Liposome Res 18:159–173

Detoni CB, Cabral-Albuquerque ECM, Hohlemweger SVA, Sampaio C, Barros TF, Velozo ES (2009) Essential oil from *Zanthoxylum tingoassuiba* loaded into multilamellar liposomes useful as antimicrobial agents. J Microencapsul 26:684–691

Dufourc E (2008) Sterols and membrane dynamics. J Chem Biol 1:63–77

El Maghraby GM, Williams AC, Barry BW (2005) Drug interaction and location in liposomes: correlation with polar surface areas. Int J Pharm 292:179–185

Elhissi AM, O'Neill MA, Roberts SA, Taylor KM (2006) A calorimetric study of dimyristoylphosphatidylcholine phase transitions and steroid–liposome interactions for liposomes prepared by thin film and proliposome methods. Int J Pharm 320:124–130

Gao D, Tang S, Tong Q (2012) Oleanolic acid liposomes with polyethylene glycol modification: promising antitumor drug delivery. Int J Nanomed 7:3517–3526

Gedara SR, Galala AA (2014) New cytotoxic spirostane saponin and biflavonoid glycoside from the leaves of *Acacia saligna* (Labill.) H.L. Wendl. Nat Prod Res 28:324–329

Habib L, Khreich N, Jraij A, Abbas S, Magdalou J, Charcosset C, Greige-Gerges H (2013) Preparation and characterization of liposomes incorporating cucurbitacin E, a natural cytotoxic triterpene. Int J Pharm 448:313–319

Habib L, Jraij A, Khreich N, Fessi H, Charcosset C, Greige Gerges H (2014) Morphological and physicochemical characterization of liposomes loading cucurbitacin E, an anti-proliferative natural tetracyclic triterpene. Chem Phys Lipids 177:64–70

Han SK, Ko YI, Park SJ, Jin IJ, Kim YM (1997) Oleanolic acid and ursolic acid stabilize liposomal membranes. Lipids 32:769–773

Heimburg T (2000) A model for the lipid pretransition: coupling of ripple formation with the chain-melting transition. Biophys J 78:1154–1165

Hu M, Konoki K, Tachibana K (1996) Cholesterol-independent membrane disruption caused by triterpenoid saponins. Biochim Biophys Acta 1299:252–258

Hunter RJ, Midmore BR, Zhang H (2001) Zeta potential of highly charged thin double-layer systems. J Colloid Interface Sci 237:147–149

Jass J, Tjarnhage T, Puu G (2000) From liposomes to supported, planar bilayer structures on hydrophilic and hydrophobic surfaces: an atomic force microscopy study. Biophys J 79:3153–3163

Juan ME, Planas JM, Ruiz-Gutierrez V, Daniel H, Wenzel U (2008) Antiproliferative and apoptosis-inducing effects of maslinic and oleanolic acids, two pentacyclic triterpenes from olives, on HT-29 colon cancer cells. Br J Nutr 100:36–43

Koukoulitsa C, Durdagi S, Siapi E, Villalonga-Barber C, Alexi X, Steele BR, Micha-Screttas M, Alexis MN, Tsantili-Kakoulidou A, Mavromoustakos T (2011) Comparison of thermal effects of stilbenoid analogs in lipid bilayers using differential scanning calorimetry and molecular dynamics: correlation of thermal effects and topographical position with antioxidant activity. Eur Biophys J 40:865–875

Lorent J, Le Duff CS, Quetin-Leclercq J, Mingeot-Leclercq JM (2013) Induction of highly curved structures in relation to membrane permeabilization and budding by the triterpenoid saponins, α- and δ-Hederin. J Biol Chem 288:14000–14017

Lou-Bonafonte J, Arnal C, Navarro M, Osada J (2012) Efficacy of bioactive compounds from extra virgin olive oil to modulate atherosclerosis development. Mol Nutr Food Res 56:1043–1057

Manez S, Recio MC, Giner RM, Rıos JL (1997) Effect of selected triterpenoids on chronic dermal inflammation. Eur J Pharmacol 334:103–105

Martín R, Ibeas E, Carvalho-Tavares J, Hernández M, Ruiz-Gutierrez V, Nieto ML (2009) Natural triterpenic diols promote apoptosis in astrocytoma cells through ROS-mediated mitochondrial depolarization and JNK activation. PLoS One 4:e5975

Martín R, Hernández M, Córdova C, Nieto ML (2012a) Natural triterpenes modulate immune-inflammatory markers of experimental autoimmune encephalomyelitis: therapeutic implications for multiple sclerosis. Br J Pharmacol 166:1708–1723

Martín R, Miana M, Jurado-López R, Martínez-Martínez E, Gómez-Hurtado N, Delgado C, Bartolomé MV, San Román JA, Cordova C, Lahera V, Nieto ML, Cachofeiro V (2012b) DIOL triterpenes block profibrotic effects of angiotensin II and protect from cardiac hypertrophy. PLoS One 7:e41545

Massey JB, Pownall HJ (2005) The polar nature of 7-ketocholesterol determines its location within membrane domains and the kinetics of membrane microsolubilization by apolipoprotein A-I. Biochemistry 44:10423–10433

Massey JB, Pownall HJ (2006) Structures of biologically active oxysterols determine their differential effects on phospholipid membranes. Biochemistry 45:10747–10758

Matsingou C, Hatziantoniou S, Georgopoulos A, Dimas K, Terzis A, Demetzos C (2005) Labdane-type diterpenes: thermal effects on phospholipid bilayers: incorporation into liposomes and biological activity. Chem Phys Lipids 138:1–11

Nishino H, Nishino A, Takayasu J, Hasegawa T, Iwashima A, Hirabayashi K, Iwata S, Shibata S (1988) Inhibition of the tumor-promoting action of ll-O-Tetradecanoylphorbol-O-acetate by some oleanane-type triterpenoid compounds. Cancer Res 48:5210–5215

Ovesna Z, Vachalkova A, Horvathova K, Tothova D (2004) Pentacyclic triterpenic acids: new chemoprotective compounds. Mini rev Neoplasma 51:327–333

Perez-Camino MC, Cert A (1999) Quantitative determination of hydroxyl pentacyclic triterpene acids in vegetable oils. J Agric Food Chem 47:1558–1562

Potamitis C, Chatzigeorgiou P, Siapi E, Viras K, Mavromoustakos T, Hodzic A, Pabst G, Cacho-Nerin F, Laggner P, Rappolt M (2011) Interactions of the AT1 antagonist valsartan with dipalmitoyl-phosphatidylcholine bilayers. Biochim Biophys Acta 1808:1753–1763

Prades J, Vögler O, Alemany R, Gomez-Florit M, Funari S, Ruiz-Gutierrez V, Barcelo F (2011) Plant pentacyclic triterpenic acids

as modulators of lipid membrane physical properties. Biochim Biophys Acta 1808:752–760

Redondo-Morata L, Giannotti MI, Sanz F (2012) Influence of cholesterol on the phase transition of lipid bilayers: a temperature-controlled force spectroscopy study. Langmuir 28:12851–12860

Reviakine I, Brisson A (2000) Formation of supported phospholipid bilayers from unilamellar vesicles investigated by atomic force microscopy. Langmuir 16:1806–1815

Richter R, Mukhopadhyay A, Brisson A (2003) Pathways of lipid vesicle deposition on solid surfaces: a combined QCM-D and AFM study. Biophys J 85:3035–3047

Rodriguez S, Garda H, Heinzen H, Moyna P (1997) Effect of plant monofunctional pentacyclic triterpenes on the dynamic and structural properties of dipalmitoylphosphatidylcholine bilayers. Chem Phys Lipids 89:119–130

Rodriguez-Rodriguez R, Perona JS, Herrera MD, Ruiz-Gutierrez V (2006) Triterpenic compounds from "orujo" olive oil elicit vasorelaxation in aorta from spontaneously hypertensive rats. J Agric Food Chem 54:2096–2102

Rodríguez-Rodríguez R, Herrera MD, Perona JS, Ruiz-Gutiérrez V (2004) Potential vasorelaxant effects of oleanolic acid and erythrodiol, two triterpenoids contained in 'orujo' olive oil, on rat aorta. Br J Nutr 92:635–642

Sánchez-Quesada C, López-Biedma A, Warleta F, Campos M, Beltrán G, Gaforio JJ (2013) Bioactive properties of the main triterpenes found in olives, virgin olive oil, and leaves of *Olea europaea*. J Agric Food Chem 61:12173–12182

Setzer WC, Setzer MC (2003) Plant-derived triterpenoids as potential antineoplastic agents. Mini Rev Med Chem 3:540–556

Sinico C, De Logu A, Lai F, Valenti D, Manconi M, Loy G, Bonsignore L, Fadda AM (2005) Liposomal incorporation of *Artemisia arborescens L.* essential oil and in vitro antiviral activity. Eur J Pharm Biopharm 59:161–168

Stiti N, Triki S, Hartmann MA (2007) Formation of triterpenoids throughout *Olea europaea* fruit ontogeny. Lipids 42:55–67

Tierney KJ, Block DE, Longo ML (2001) Elasticity and phase behavior of DPPC membrane modulated by cholesterol, ergosterol, and ethanol. Biophys J 89:2481–2493

Valenti D, De Logu A, Loy G, Sinico C, Bonsignore L, Cottiglia F, Garau D, Fadda AM (2001) Liposome-incorporated *Santolina insularis* essential oil: preparation, characterization and in vitro antiviral activity. J Liposome Res 11:73–90

Verma DD, Verma S, Blume G, Fahr A (2003) Particle size of liposomes influences dermal delivery of substances into skin. Int J Pharm 258:141–151

Yang G, Chen B, Zhang Z, Gong J, Bai H, Li J, Wang Y, Li B (2009) Cytotoxic activities of extracts and compounds from viscum coloratum and its transformation products by *Rhodobacter sphaeroides*. Appl Biochem Biotechnol 152:353–365

Yoshida PA, Yokota D, Foglio MA, Rodrigues RAF, Pinho SC (2010) Liposomes incorporating essential oil of Brazilian cherry (*Eugenia uniflora L.*): characterization of aqueous dispersions and lyophilized formulations. J Microencapsul 27:416–425

Zhao L, Feng SS (2005) Effects of lipid chain unsaturation and headgroup type on molecular interactions between paclitaxel and phospholipid within model biomembrane. J Colloid Interface Sci 285:326–335